

# Exploration of Human Serum Albumin Binding Sites by Docking and Molecular Dynamics Flexible Ligand–Protein Interactions

Omar Deeb,<sup>1</sup> Martha Cecilia Rosales-Hernández,<sup>2</sup> Carlos Gómez-Castro,<sup>2</sup> Ramón Garduño-Juárez,<sup>3</sup> José Correa-Basurto<sup>2</sup>

<sup>1</sup> Faculty of Pharmacy, Al-Quds University, Jerusalem, Palestine

<sup>2</sup> Laboratorio de Modelado Molecular-SEPI y Departamento de Bioquímica de la Escuela Superior de Medicina del Instituto Politécnico Nacional, Plan de San Luis y Díaz Mirón s/n, México D.F.11340, México

<sup>3</sup> Instituto de Ciencias Físicas, Universidad Nacional Autónoma de México, PO Box 48-3, Cuernavaca, Morelos 62250, México

Received 11 July 2009; revised 11 September 2009; accepted 12 September 2009

Published online 25 September 2009 in Wiley InterScience (www.interscience.wiley.com). DOI 10.1002/bip.21314

## ABSTRACT:

Five-nanosecond molecular dynamics (MD) simulations were performed on human serum albumin (HSA) to study the conformational features of its primary ligand binding sites (I and II). Additionally, 11 HSA snapshots were extracted every 0.5 ns to explore the binding affinity ( $K_d$ ) of 94 known HSA binding drugs using a blind docking procedure. MD simulations indicate that there is considerable flexibility for the protein, including the known sites I and II. Movements at HSA sites I and II were evidenced by structural analyses and docking simulations. The latter enabled the study and analysis of the HSA–ligand interactions of warfarin and ketoprofen (ligands binding to sites I and II, respectively) in greater detail. Our results indicate that the free energy values by docking ( $K_d$  observed) depend upon the conformations of both HSA and the ligand. The 94 HSA–ligand binding  $K_d$  values, obtained by the docking procedure, were

subjected to a quantitative structure–activity relationship (QSAR) study by multiple regression analysis. The best correlation between the observed and QSAR theoretical ( $K_d$  predicted) data was displayed at 2.5 ns. This study provides evidence that HSA binding sites I and II interact specifically with a variety of compounds through conformational adjustments of the protein structure in conjunction with ligand conformational adaptation to these sites. These results serve to explain the high ligand–promiscuity of HSA. © 2009 Wiley Periodicals, Inc. *Biopolymers* 93: 161–170, 2010.

**Keywords:** human serum albumin; molecular dynamics; docking; multiple linear regression analysis

This article was originally published online as an accepted preprint. The “Published Online” date corresponds to the preprint version. You can request a copy of the preprint by emailing the *Biopolymers* editorial office at [biopolymers@wiley.com](mailto:biopolymers@wiley.com)

Additional Supporting Information may be found in the online version of this article.

Correspondence to: José Correa-Basurto; e-mail: [jcorreab@ipn.mx](mailto:jcorreab@ipn.mx) or Omar Deeb; e-mail: [deeb2000il@yahoo.com](mailto:deeb2000il@yahoo.com)

Contract grant sponsor: CONACYT

Contract grant number: 62488

Contract grant sponsor: COFAA-SIP/IPN

Contract grant number: 20090618

Contract grant sponsor: CONACYT

Contract grant number: 46061-R

© 2009 Wiley Periodicals, Inc.

## INTRODUCTION

Proteins are macromolecules consisting of different numbers and sequences of amino acids, which allow them to adopt different 3D structures and possess unique biological functions. Among the most important of these biological functions are biochemical reaction catalysis, cellular signal generation, ligand transport, and structural support. The overall protein structure is flexi-

ble under natural conditions. As such, it is possible that regulatory proteins have different binding sites and undergo ligand-binding site conformational changes during the process of ligand binding.<sup>1</sup> However, it has been shown that some monomeric proteins are capable of binding to several ligands at different sites.<sup>2</sup> These types of proteins have been termed “ligand promiscuous.” This behavior is a feature of human serum albumin (HSA), the most abundant plasma protein, and is characterized by its surprising capacity to bind a large variety of biologically active molecules.<sup>3</sup>

The reason for the high degree of promiscuity of HSA remains unclear.<sup>4</sup> Therefore, promiscuous proteins, such as HSA and HIV-1 reverse transcriptase, have been the subject of an intense scientific debate that is centered around whether drugs can bind to several protein targets unselectively or in specific forms.<sup>5</sup> It has been proposed that promiscuous protein activity, in contrast to nonpromiscuous proteins, is predominantly entropy driven, excluding pair-wise enthalpy interactions.<sup>6</sup> As such, a deeper understanding of the physiochemical and structural properties of HSA may serve to better elucidate the behavior of these promiscuous proteins. It is well known that the formation of a ligand–protein complex depends on atomic charge, steric hindrance, and hydrophobic properties.<sup>7,8</sup> A recent study demonstrated that inducing conformational disorder may serve to enhance drug affinity in the protein–drug association process.<sup>9</sup> Thus, HSA protein movements could permit a degree of plasticity, which in turn might be directly related to a myriad of functions and binding properties that could be used to design new protein carriers for drugs.<sup>10</sup>

During the course of drug design, it is important to fully understand the conformational barriers involved in the ligand–target recognition process. Such a task can be achieved through several techniques, including X-ray crystallography, nuclear magnetic resonance (NMR) spectroscopy, and scanning electron microscopy (SEM). Additionally, computational methods, such as molecular dynamics (MD) simulations, can be used. MD is a computational method commonly used to generate multiple target conformations, allowing significant backbone and amino acid side chain rearrangements.<sup>11,12</sup> It has also been shown that MD yields better data when mixed with docking simulations that allow for the visualization of ligand recognition behavior and for the analysis of free energy values, in comparison with experimental results.<sup>13</sup>

While X-ray, NMR, and SEM experiments can show ligand–protein interactions with a high level of molecular detail, theoretical binding energy calculations by docking methods can be used to analyze biological processes rapidly and efficiently. These also enable the calculation of molecular

interaction free energy values.<sup>14</sup> Molecular docking is widely used in drug discovery to aid in understanding the molecular interactions involved in protein–ligand binding. Historically, docking protocols have considered both the ligand and protein, in rigid structure form, as adequate representations of the protein.<sup>15</sup> Subsequently, the ligand is treated as a flexible entity.<sup>16</sup> However, this method typically does not take into account protein side chains, which are generally more disordered than those in the backbone. As a result, flexible target/ligand models have been proposed where multiple side chain conformers are generated, while maintaining fixed backbone atoms.<sup>17</sup> Other newer models have introduced a more accurate description by introducing protein flexibility and its influence on ligand recognition.<sup>18–20</sup>

In the present study, MD and docking techniques were combined to evaluate the binding of 94 different HSA drugs, which were reported by Colmenarejo et al.<sup>21</sup> (see Supporting Information: Table I-S), on 11 HSA snapshots. These were extracted every 0.5 ns, during 5 ns of MD simulation, and were performed using both solvated and ionized HSA conditions. These studies facilitated the evaluation of the contribution of HSA conformational changes toward its protein promiscuity. A subset of analyses focused specifically on protein–ligand interactions of warfarin and ketoprofen.<sup>22</sup> All docking results were validated by a quantitative structure–activity relationship (QSAR) performed using the multiple linear regression modeling method.

## MD PROTOCOL

Classical MD simulations were carried out using the NAMD 2.6 program<sup>23</sup> using the CHARMM27 force field.<sup>24</sup> Starting HSA coordinates were taken from the 1.9 Å resolution crystal structure of Wardell M. et al., (PDB ID: 1n5u).<sup>25</sup> The included heme group, myristic acid, and water molecules of the crystal structure were removed. Hydrogen atoms were added by using the psfgen program included in the VMD package.<sup>26</sup> Next, this structure was neutralized with 14 sodium ions after being immersed in a TIP3P water box containing 22,604 water molecules. The equilibration protocol began with 1500 minimization steps followed by 30 ps of MD at 310 K with fixed protein atoms. Then, the entire system was minimized for 1500 steps (at 0 K) and then heated gradually from 10 to 310 K by temperature reassignment during the first 60 ps of a 100-ps equilibration dynamics, without restraints.<sup>27</sup> The final step was a 30 ps NTP dynamics using the Nose-Hoover Langevin piston pressure control<sup>28</sup> at 310 K and 1.01325 bar for density (volume) fitting. From this point, the simulation was continued in the NTV ensemble for 5 ns. Periodic boundary conditions and the

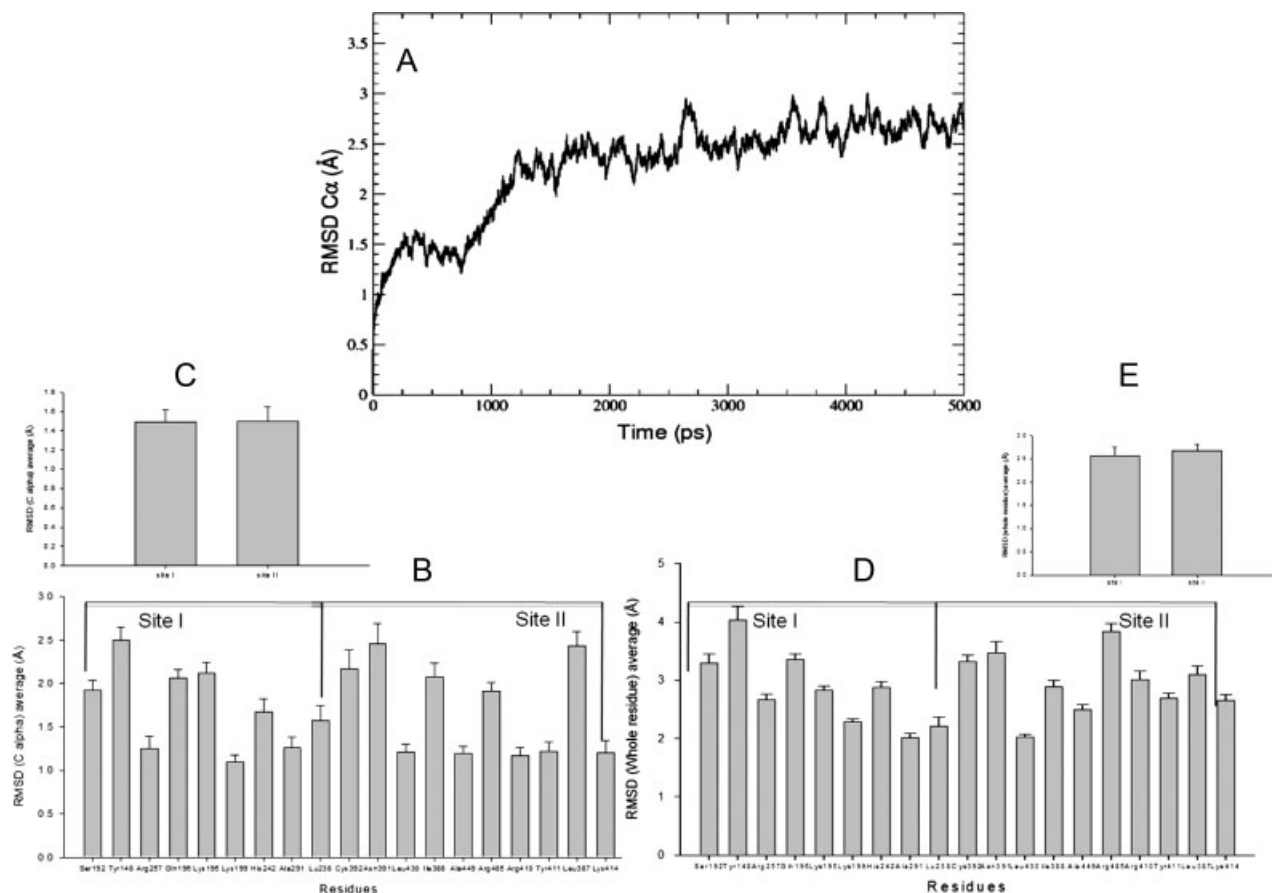


**FIGURE 1** (A) The  $\alpha$ -carbon root mean square distance (RMSD) for HSA during 5 ns of MD simulations and the time averaged (B)  $\alpha$ -carbon and (D) whole RMSD for residues of binding sites I and II. Comparisons are given in (C) and (E).

particle-mesh Ewald method<sup>29</sup> were applied for a complete electrostatics calculation. The dielectric water constant was used, and the temperature was maintained at 310 K using Langevin dynamics. Nonbonded interactions were calculated by applying a 10 Å cutoff, with a switching function at 8 Å. The nonbonded list generation was stopped at 11.5 Å. The SHAKE method<sup>30</sup> was used to provide an integration time step of 2 fs, while keeping all bonds to hydrogen atoms rigid.

The trajectory was stored every 1 ps and further analyzed with the VMD program.<sup>26</sup> The MD simulation output over 5 ns provided several HSA structures that were sampled every 0.5 ns (see Figure 1) to study the ligand recognition energetic and binding modes of 94 well-known ligands.<sup>21</sup>

## DOCKING PROTOCOL

Geometry optimization of the ligands reported by Colmenarejo<sup>21</sup> was performed by HYPERCHEM (Version 7.0, Hypercube, USA, <http://www.hyper.com>) at the AM1 level. The AutoDock (3.0.5) program was selected for docking

studies, as this algorithm maintains a rigid macromolecule while allowing ligand flexibility.<sup>16</sup> This program has been used widely because it displays good free energy correlation values between docking simulations (observed) and experimental data.<sup>31</sup> This program begins with a ligand molecule in an arbitrary conformation, orientation, and position. It identifies the most energetically favorable ligand-HSA complexes by using both simulated annealing and genetic algorithms. A GRID-based procedure was utilized to prepare structural inputs and to define all binding sites.<sup>32</sup> A rectangular lattice (126 × 126 × 126 Å), with points separated by 0.375 Å, was superimposed on the entire protein structure following a blind docking procedure.<sup>33</sup>

All docking simulations were conducted using the hybrid Lamarckian genetic algorithm, with an initial population of 100 randomly placed individuals and a maximum of  $1.0 \times 10^7$  energy evaluations. All other parameters were maintained at their default settings. The resulting docked orientations within a root mean square deviation of 0.5 Å were clustered together. The lowest energy cluster for each ligand was sub-

jected to further free energy values and binding geometric analyses, as previously reported.<sup>34</sup>

## MOLECULAR DESCRIPTORS

Chemical structures of the 94 HSA drug and drug-like compounds reported by Colmenarejo<sup>21</sup> were obtained from the National Center for Biotechnology Information (available at: <http://pubchem.ncbi.nlm.nih.gov/search>). These structures were optimized at the AM1 level of semiempirical theory using the HYPERCHEM software program. The AM1 geometry optimizations were preceded by the Polak-Rebire algorithm to reach a 0.01 root mean square gradient (298 K, gas phase). Esbelen (compound number 8, see Supporting Information Table I-S) was removed from this set, as selenium (Se) is not parameterized in the AM1 semiempirical method. In this study, a set of 60 molecular descriptors was calculated using the HYPERCHEM and DRAGON software programs (see Supporting Information Table II-S). These descriptors include constitutional, topological, chemical, and quantum descriptors.

## QSAR ANALYSIS

QSAR analysis of docking results was performed using multiple linear regression analysis with stepwise selection and elimination of variables. This was carried out to model the observed and theoretical binding affinity ( $\log K_d$  values) relationships with a set of 60 descriptors. Some compounds were removed, due to large  $\Delta G$  values (unrealistic  $K_d$  values), and other outliers were discarded from the principal component analysis.<sup>4</sup> As such, the relationship analysis between observed and docking-calculated  $\log K_d$  values was conducted for a set of 78 ligands. Multilinear regression models and cross-validation parameters at different time values ( $t$ ) are shown in Supporting Information (Figures 1-S and 2-S, Tables III-S and IV-S), and a key for descriptor abbreviations used in this study is provided in Supporting Information (Table II-S).

## RESULTS AND DISCUSSION

### Molecular Dynamic Simulations

In this study, we used combined MD/docking approaches to estimate the binding affinities of several HSA ligands and subsequently carried out QSAR analyses using several ligand properties. The overall goal of the MD simulation was to provide a more refined and flexible HSA structure model for use during the docking procedure, as shown by Alonso et al.<sup>35</sup> The procedure was carried out while accounting for

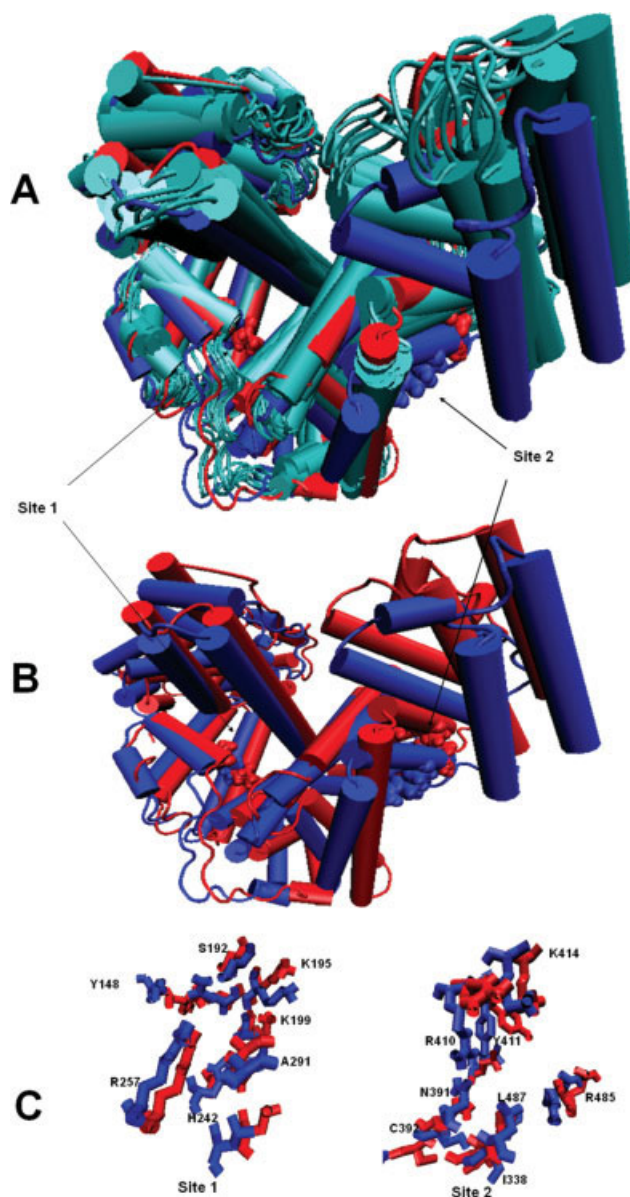


**FIGURE 2** (A) All HSA conformer structures from MD simulations, from 0 to 5 ns in 0.5 ns increments. (B) HSA conformer structures at 0 and 5 ns. (C) HSA binding sites (I and II) at 0 and 5 ns. In this figure, the blue coloring = 0 ns and red coloring = 5 ns.

certain physiological and environmental factors that occur on proteins, which are not considered in simpler docking protocols.<sup>16</sup> This is mainly because 3D protein structures placed in the Protein Data Bank must be corrected for unnatural features, such as bad contacts or missing atoms. Relaxation of the 3D structure is required when using the solid-state X-ray in order to obtain conformations adequate for performing the required docking simulations. This can be achieved by an MD simulation of protein flexibility (see Figure 2) taking into account conformational changes in the

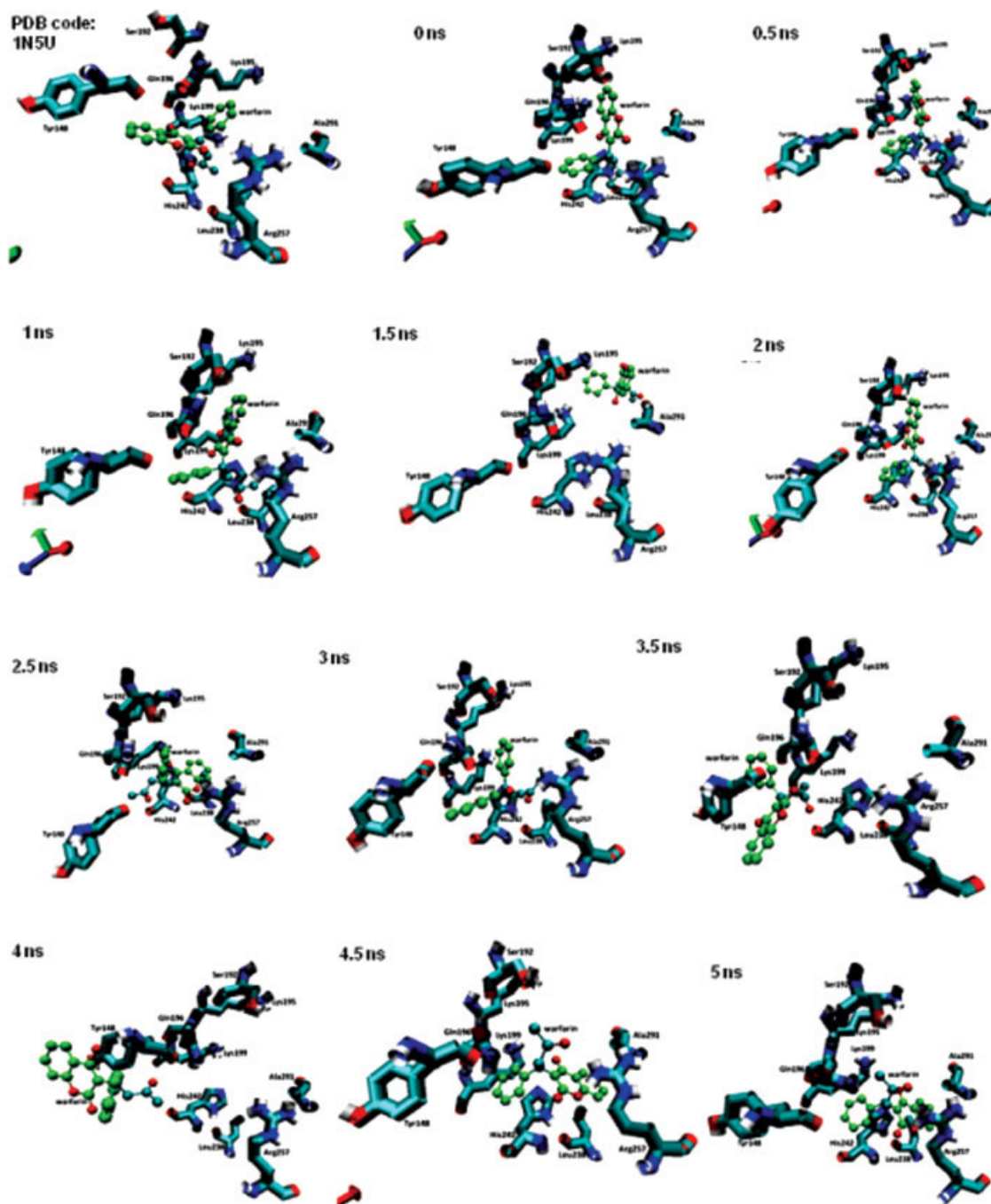


FIGURE 3 Docking interactions of warfarin at site I of all HSA MD snapshots sampled.

binding site region, due to the mobility of its neighboring protein regions and the intrinsic backbone flexibility of some amino acid residues.<sup>36</sup> It is important to consider this fact for ligand recognition processes, to improve theoretical binding energies by computational docking methods. However, theoretical methods do not consider many factors involved in ligand–target recognition, which are certainly beyond the chemical composition of the ligand.

The plot of the backbone  $\alpha$ -carbon root mean square distance (RMSD  $C\alpha$ , Figure 1A) shows a structural transition during the 5 ns of MD simulation for the whole protein. This is maintained for the first 2 ns, when the RMSD  $C\alpha$  is raised from 1.3 to 2.5 Å, reaching  $\sim 3.0$  Å at some points during the remainder of the simulation. It is well known that HSA possesses two primary ligand binding sites (I and II). These binding sites have been identified by X-ray crystallographic

**Table I** Free Energy ( $\Delta G$ ) Values of Warfarin and Ketoprofen at Sites I and II, Respectively, on All HSA Structures Generated by MD (5 ns)

$t$ (ns)	Warfarin <sup>b</sup> ( $\Delta G$ , Kcal/mol)	Ketoprofen <sup>c</sup> ( $\Delta G$ , Kcal/mol) <sup>a</sup>
pdb code: 1N5U	-8.13	-9.6
0	-7.66	-8.84
0.5	-7.54	-6.33
1	-7.7	-6.24
1.5	-6.93	-6.35
2	-7.23	-7.19
2.5	-7.38	-6.10
3	-7.12	-6.3
3.5	-7.78	-6.29
4	-7.62	-6.38
4.5	-7.19	-6.43
5	-7.77	-6.13

<sup>a</sup> Docking values at HSA site II.<sup>b</sup> Compound 53 in Table 1-S (Supporting Information).<sup>c</sup> Compound 59 in Table 1-S (Supporting Information).

analysis, fluorescence, affinity chromatography, calorimetric analysis, circular dichroism, and other experimental techniques, some of which have yielded ligand–protein affinities. Sudlow's nomenclature places site I in HSA subdomain IIA, where bulky heterocyclic anions prefer to bind, whereas site II is placed in subdomain IIIA, which is preferred by aromatic carboxylates.<sup>37,38</sup> To date, two of the most studied HSA ligands are warfarin and ketoprofen. It is known that binding site I is selective for warfarin,<sup>39</sup> whereas binding site II is selective for ketoprofen.<sup>40,41</sup> The majority of the residues that comprise both binding sites shows an averaged RMSD C $\alpha$  ( $\sim 3$  ns) for the entire simulation, as illustrated in Figures 1B and 1C. In the case of binding site I, Ser193, Tyr148, Gln196, and Lys195 show higher mobilities compared with the remaining residues (Figures 1B and 1D). Although the side chain of Tyr148 is relatively far from the binding pocket, the side chains of Lys199, Arg257, and His242 are in direct contact with the ligands (see Figure 3). As such, their movements would likely affect the estimated affinities for the ligands over the time course of the MD simulation. Thus, these could be direct determinants of the ability of this site to bind to structurally diverse ligands (see Table I). Apparently, the residues of binding site II displayed lower mobilities compared to site I (Figures 1B and 1D). However, this is untrue, as their entire movement was not different (see Figures 1C and 1E). Only Asn391 and Leu387 showed an RMSD C $\alpha$ . Asn391 and Arg485 (whole residue) averaged significantly higher than other residues, which could be due to its proximity to the protein surface. This would allow it to

make hydrogen bonding interactions with surrounding water molecules, except for Leu387. These significant structural movements showed different affinity values with ketoprofen (Table I).

MD simulations indicate that there is significant movement for the protein as a whole (Figure 2A), but little movement at sites I and II, according to structural evaluations (Figures 2B and 2C). These HSA movements were corroborated by RMSD C $\alpha$  deviation at sites I and II (Figures 1C and 1E). Such protein flexibility has been associated with changes in protein function and ligand binding.<sup>42,43</sup> This was observed for HSA, as several HSA subdomain movements significantly modified binding site behavior. HSA displayed several structural movements, but it maintained its 3D structure (not unfolded) under certain pathologies that alter pH, ionic properties, and osmotic blood properties. This is likely due to the great number of disulfide Cys-Cys bonds<sup>17</sup> possessed by this protein. Thus, HSA movements are not sufficient to unfold the protein (see Figure 2), reproducing the environmental behavior of HSA. The results of this work suggest that HSA flexibility underlies the preferential affinity for several ligands by this protein, as has been observed for other known promiscuous proteins, such as CYP450 and chloroperoxidase.<sup>44,45</sup> These MD simulations support the idea that HSA displays conformational movements that modify several molecular properties and allow it to bind to several ligands at different times or even at the same time.<sup>46</sup> This supports the notion that the HSA protein is ligand promiscuous, as it shows several binding sites at different time points within movements that conserve its 3D structure.

## Docking

The 11 HSA structures, sampled every 0.5 ns during 5 ns of MD simulation, were used in docking studies with 94 well-known ligands, including warfarin<sup>39</sup> and ketoprofen.<sup>40</sup> These ligands, in particular, were selected to explore the recognition behavior for known binding sites I and II, respectively (Figures 3 and 4). The docking free energy values for each of the complexes, expressed as an empirical free energy potential, are shown in Table I for these two compounds. The relative docking orientations of warfarin with respect to the 11 superimposed structures of HSA binding site I are shown in Figure 3. A similar picture of the relative orientations of ketoprofen with respect to the 11 superimposed structures of HSA binding site II is shown in Figure 4. These figures highlight the interdependence of HSA binding site conformation and ligand orientation. In both figures, the backbone and side chain movements of the residues involved in ligand recognition at different times (ns), with respect to the native

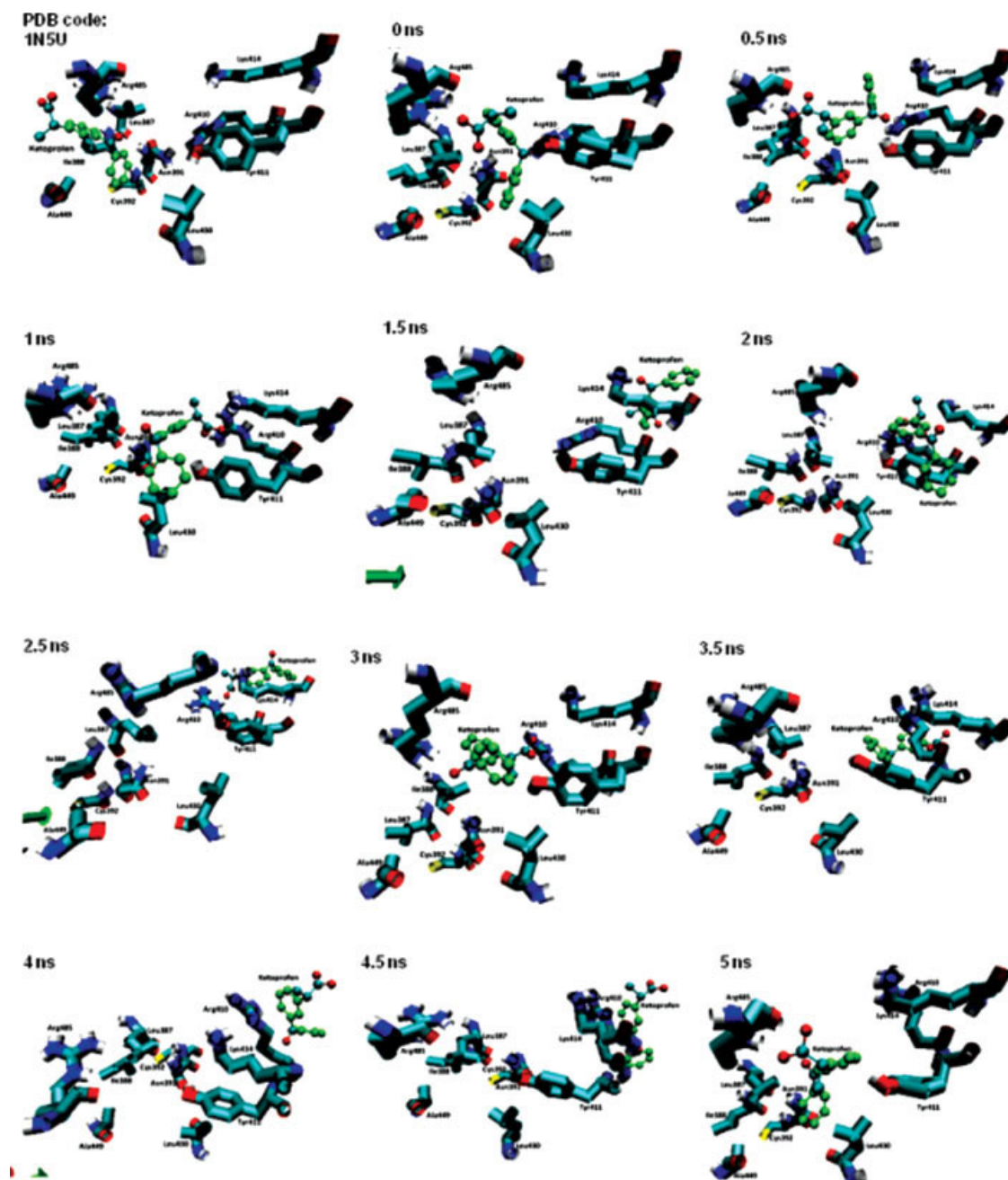


FIGURE 4 Docking interactions of ketoprofen at site II of all HSA MD snapshots sampled.

HSA structure (pdb core, 1N5U), are depicted. As such, it is evident that both binding sites showed considerable flexibility despite a significantly higher degree of motility for the remainder of the protein (Figures 2A and 2C).

These HSA domain and binding site movements enable ligands to adopt different structural binding modes (see Figures 3 and 4) and, consequently, different free energy values (Table I). This process is facilitated by changes in the relative orientations of amino acids at the binding sites. These subsequently induce changes in local physicochemical prop-

erties, such as hydrophobicity, steric hindrance effects, and electronic distributions. Therefore, it is not surprising that the net effect is a modification of the ligand affinities toward proteins and protein–protein interactions.<sup>47</sup>

Although Sudlow's classification of the binding sites remains useful,<sup>48</sup> some high-affinity drugs do not show specific preference for site I or II and could simply be binding to other regions of the HSA molecule (unpublished data). Site I, also known as the warfarin binding site, is formed by a pocket located in subdomain IIA of HSA.<sup>38</sup> Site I accepts

ligands that have dicarboxylic acids and/or bulky heterocyclic molecules that are characterized by a negative centrally localized charge. This could be due to the presence of Arg257 and Lys195/199 residues at this binding site, which confer a partial positive character.<sup>49</sup> The docking results shown in Figure 3 indicate that warfarin makes several interactions with these residues, including:  $\pi$ -cation interactions between aromatic moieties of the ligand and the Arg/Lys side chain amine group; hydrogen bonding interactions between the hydroxyl group of Ser192 and oxygen atoms of warfarin, during snapshots taken at 4.5 and 5 ns; and  $\pi$ - $\pi$  interactions with the aromatic system of Tyr148, during snapshots taken at 3.5 and 4 ns (see Figure 3).

Binding site II is located in subdomain IIIA of HSA and is known as the benzodiazepine binding site. In addition, ibuprofen, diazepam, phenylbutazone, and ketoprofen selectively bind to this site.<sup>50</sup> Ligands bound to site II are characterized by aromatic moieties and carboxylic acids bearing a negatively charged carboxylate group at the end of the molecule, away from a hydrophobic center. As previously reported, binding site II accepts fewer ligands than site I, which could be because site II is located in a subdomain that corresponds to a more unstable protein conformation (see Figure 2A) relative to site I. As a consequence, this small binding site accepts ligands that display lower overall affinities, as was identified for ibuprofen by displacement of oleic acid.<sup>51</sup> This observation is consistent with our findings (see Table I). Figure 4 demonstrates that ketoprofen binds to HSA binding site II through several  $\pi$ -cation interactions between the basic side chain residue of Arg410, at snapshots taken at 1.5, 2, 2.5, 3.5, 4, and 4.5 ns, and Arg485, at snapshots taken at 3 ns, whereas Lys414, at snapshots of 1.5, 2, 2.5, 3.5, and 4.5 ns, interacts with the aromatic system of ketoprofen. Additionally,  $\pi$ - $\pi$  interactions between the aromatic moiety of this ligand and Tyr411 are also present at snapshots taken at 1 and 2 ns.

Aromatic clusters have been reported to play an important role in molecular recognition.<sup>52</sup> This behavior can be corroborated by either experimental procedure or theoretical simulation. One of these theoretical methodologies involves docking studies that simulate amino acid side chain movement.<sup>18</sup> This procedure does not likely take into consideration the important role that the whole protein movement plays in the ligand recognition process (see Table I). Figure 2 shows small HSA movements at binding site I, as predicted by docking simulations. However, there is evidence that these conformational changes can influence ligand recognition in different binding geometries and with different free energies of binding due to changes in the overall chemical environment. This indicates that minimum protein movements can display different binding site properties, allowing several

ligand affinities with the same ligand at different time snapshots, as was observed in pyruvate kinase.<sup>53</sup>

Table I shows how the free energy values of warfarin and ketoprofen docked in HSA. These free affinity values varied with the individual protein structure sampled at different simulation times (5 ns), indicating that the HSA free affinity values for these ligands depend on both protein and ligand movements (Figures 2–4). These results are consistent with the observation that site I is more selective for warfarin, whereas site II is more selective for ketoprofen, in agreement with reported data.<sup>39,40</sup>

### MD-QSAR Models of Drug Binding to HSA

Our work uses theoretical methods (docking and MD simulations), but few of these models have been explored for protein–ligand interaction values.<sup>19,20</sup> We carried out a QSAR study by using the ligand descriptor versus  $K_d$  values, which were obtained by docking simulations (observed), to obtain the  $K_d$  values (predicted). Table IV-S (Supporting Information) shows cross-validation parameters for the models obtained at different  $t$  values in the 5 ns range. This table indicates that the model obtained at  $t = 2.5$  ns had the lowest relative prediction error, the lowest standard error of prediction, and the lowest predictive residual sum of squares value. As a result, this QSAR model was selected as optimal relative to all others. The calibration and cross-validation coefficients of determination for this model were 0.889 and 0.875, respectively. This indicates that this model can at least explain the 88.9% and 87.5% variances in the  $\log K_d$  for the calibration and prediction, respectively. Figure 5 shows the predicted and observed  $\log K_d$  values, along with their residuals for this model.

The regression equation for this model was provided by:

$$\begin{aligned} \log K_d = & 2.230 (\pm 2.906) + 0.207 (\pm 0.199) \\ & \text{nCIC} - 0.008 (\pm 0.018) \text{nAT} + 0.008 (\pm 0.002) \\ & \text{W} - 0.023 (\pm 0.011) \text{Ref} - 0.046 (\pm 0.029) \\ & \text{nHDon} - 0.051 (\pm 0.020) \text{DMt} - 8.777 (\pm 5.156) \\ & \text{PW2} - 0.002 (\pm 0.000) \text{SMTI} - 0.035 (\pm 0.032) \\ & \log P - 0.003 (\pm 0.001) \text{HF} - 0.357 (\pm 0.164) \times 2 \\ & + 0.826 (\pm 0.334) \text{MNC} + 0.023 (\pm 0.011) \text{HE} \\ & + 4.151 (\pm 3.434) \text{PW4} + 0.021 (\pm 0.015) \text{DMx} \\ & + 0.002 (\pm 0.002) \text{ZM2V}, \end{aligned}$$

where  $N = 78$ ,  $R^2 = 0.889$ ,  $R_{CV}^2 = 0.875$ ,  $\text{PRESS} = 6.960$ ,  $S_{\text{PRESS}} = 0.338$ ,  $\text{PSE} = 0.299$ , and  $\text{RSEP} = 5.090\%$ . Here,  $N$  is the number of compounds,  $R^2$  is the coefficient of determination,  $R_{CV}^2$  is the cross-validation coefficient of determina-

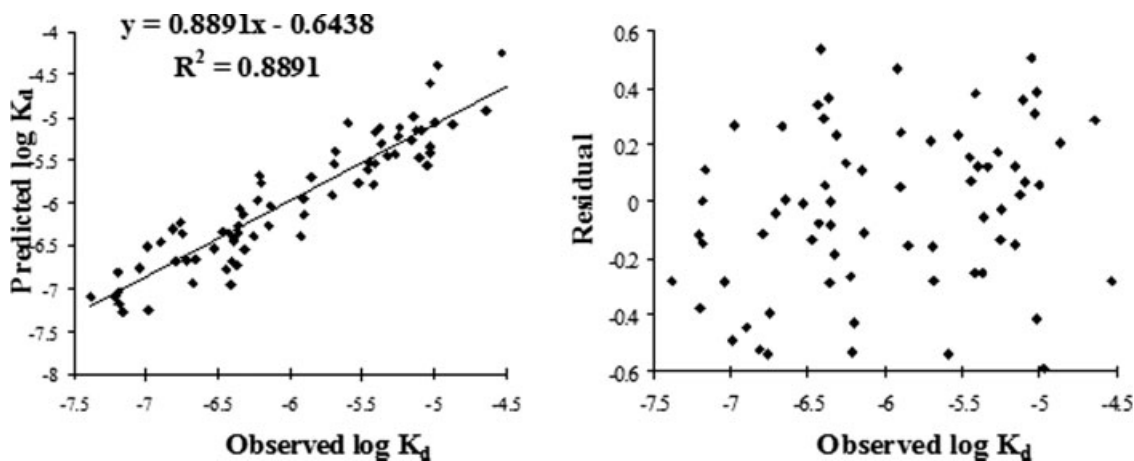


FIGURE 5 Predicted docking affinity versus observed docking affinity (left) and corresponding residual (right) obtained by MD simulations for the best QSAR model obtained ( $t = 2.5$  ns).

tion, PRESS is the predictive residual sum of squares,  $S_{\text{PRESS}}$  is the uncertainty of prediction, PSE is the standard error of prediction, and RSEP is the relative standard error of prediction.

The above equation shows that the most significant descriptor is the topological descriptor PW2 (path/walk-2-randic shape index), where  $\log K_d$  is inversely proportional to PW2. Another significant descriptor is PW4 (path/walk-4-randic shape index), where increasing the PW4 value raises the  $\log K_d$  value. This means that a greater ligand surface, in general, increases the protein surface contact on HSA because of an increase in the number of interactions. This phenomenon has been widely described for small-protein interactions.<sup>54</sup>

## CONCLUSIONS

We have demonstrated that the combination of MD and docking procedures provides the best fit for protein–ligand complexes. This was corroborated and validated with subsequent QSAR studies. The results of this study indicate that HSA movements play an important role in drug recognition. Although conformational changes were minimal at HSA binding sites I and II, docked warfarin and ketoprofen displayed significantly different interactions. As such, this approach was able to identify the HSA structures involved in the recognition process and explains HSA promiscuity. In addition, this study has also facilitated the identification of chemical property changes on several HSA structures that resulted in different docking energy affinities.

This study illustrates that molecular docking/dynamics can provide a useful and accurate picture of protein–ligand interactions at the molecular level. This is because MD mimics certain key physiological conditions including pH, ion content, solvation, and temperature. As such, it is a good

option in studying and explaining the molecular basis of simultaneous protein recognition selectivity. These computational techniques can also explain the molecular basis of pharmacologically important events that involve binding site recognition on HSA sites II and I in drug displacement.

The authors thank Ian Ilizaliturri Flores for building and supporting two clusters (6 and 20 nodes) used in the MD and docking simulations at ESM-IPN.

## REFERENCES

- Ota, N.; Agard, D. A. *J Mol Biol* 2001, 314, 607–617.
- Torres, E.; Aburto, J. *Arch Biochem Biophys* 2005, 437, 224–232.
- Bertucci, C.; Andrisano, V.; Gotti, R.; Cavrini, V. *J Chromatogr B* 2002, 768, 147–155.
- Deeb, O.; Hemmateenejad, B. *Chem Biol Drug Des* 2007, 70, 19–29.
- Fernández, A.; Tawfik, D. S.; Berkhout, B.; Sanders, R.; Kloczkowski, A.; Sen, T.; Jernigan, B. *J Biomol Struct Dyn* 2005, 22, 615–624.
- Nobeli, I.; Favia, A. D.; Thornton, J. M. *Nat Biotechnol* 2009, 27, 157–167.
- Kundu, S.; Jernigan, R. L. *Biophys J* 2004, 86, 3846–3854.
- Lill, M. A.; Vedani, A.; Dobler, M. *J Med Chem* 2004, 47, 6174–6186.
- Crespo, A.; Fernández, A. *Mol Pharm* 2008, 5, 430–437.
- Kratz, F. *J Control Release* 2008, 132, 171–183.
- McGee, T. D.; Edwards, J.; Roitberg, A. E. *Int J Environ Res Public Health* 2008, 5, 111–114.
- Arinaminpathy, Y.; Sansom, M. S. P.; Biggin, P. C. *Biophys J* 2002, 82, 676–683.
- Talele, T. T.; McLaughlin, M. L. *J Mol Graph Model* 2008, 26, 1213–1222.
- Huang, B.; Schroeder, M. *Gene* 2008, 422, 14–21.
- Li, L.; Chen, R.; Weng, Z. *Proteins* 2003, 53, 693–707.
- Morris, G. M.; Goodsell, D. S.; Halliday, R. S.; Huey, R.; Hart, W. E.; Belew, R. K.; Olson, A. J. *J Comp Chem* 1998, 19, 1639–1662.

17. Hartmann, C.; Antes, I.; Lengauer, T. *Proteins* 2009, 74, 712–726.
18. Kokh, D. B.; Wenzel, W. *J Med Chem* 2008, 51, 5919–5931.
19. Król, M.; Chaleil, R. A.; Tournier, A. L.; Bates, P. A. *Proteins* 2007, 69, 750–757.
20. Pyrkov, T. V.; Kosinsky, Y. A.; Arseniev, A. S.; Priestle, J. P.; Jacoby, E.; Efremov, R. G. *J Chem Inf Model* 2007, 47, 1171–1181.
21. Colmenarejo, G.; Alvarez-Pedraglio, A.; Lavandera, J. L. *J Med Chem* 2001, 44, 4370–4378.
22. Wang, H.; Hanfa, Z.; Yukui, Z. *Sci China B* 1997, 40, 643–649.
23. Phillips, J. C.; Braun, R.; Wang, W.; Gumbart, J.; Tajkhorshid, E.; Villa, E.; Chipot, C.; Skeel, R. D.; Kale, L.; Schulten, K. *J Comp Chem* 2005, 26, 1781–1802.
24. MacKerell, A. D., Jr.; Bashford, D.; Bellott, M.; Dunbrack, R. L., Jr.; Evanseck, J.; Field, M. J.; Fischer, S.; Gao, J.; Guo, H.; Ha, S.; Joseph, D.; Kuchnir, L.; Kuczera, K.; Lau, F. T. K.; Mattos, C.; Michnick, S.; Ngo, T.; Nguyen, D. T.; Prodhom, B.; Reiher, I. W. E.; Roux, B.; Schlenkrich, M.; Smith, J.; Stote, R.; Straub, J.; Watanabe, M.; Wiorkiewicz-Kuczera, J.; Yin, D.; Karplus M. *J Phys Chem B* 1998, 102, 3586–3616.
25. Wardell, M.; Wang, Z.; Ho, J. X.; Robert, J.; Ruker, F.; Ruble, J.; Carter, D. C. *Biochem Biophys Res Commun* 2002, 291, 813–819.
26. Humphrey, W.; Dalke, A.; Schulten, K. *J Mol Graph* 1996, 14, 33–38.
27. Espinoza-Fonseca, L. M.; Trujillo-Ferrara, J. G. *Biopolymers* 2006, 83, 365–373.
28. Martyna, G. J.; Tobias, D. J.; Klein, M. L. *J Chem Phys* 1994, 101, 4177–4189.
29. Batcho, P. F.; Case, D. A.; Schlick, T. *J Chem Phys* 2001, 115, 4003–4018.
30. Ryckaert, J. P.; Ciccotti, G.; Berendsen, H. J. C. *J Comput Phys* 1977, 23, 327–314.
31. Gorelik, B.; Goldblum, A. *Proteins* 2008, 71, 1373–1386.
32. Goodford, P. J. *J Med Chem* 1985, 28, 849–857.
33. Hetényi, C.; van der Spoel, D. *FEBS Lett* 2006, 580, 1447–1450.
34. Correa-Basurto, J.; Flores-Sandoval, C.; Marín-Cruz, J.; Rojo-Domínguez, A.; Espinoza-Fonseca, L. M.; Trujillo-Ferrara, J. G. *Eur J Med Chem* 2007, 42, 10–19.
35. Alonso, H.; Bliznyuk, A. A.; Gready, J. E. *Med Res Rev* 2006, 26, 531–568.
36. Holyoake, J.; Sansom, M. S. *Structure* 2007, 15, 873–884.
37. Peters, T. *All About Albumin: Biochemistry, Genetics and Medical Applications*; Academic Press: San Diego, CA, 1966.
38. He, X. M.; Carter, D. C. *Nature* 1992, 358, 209–215; Erratum in: *Nature* 1993, 364, 362.
39. Petitpas, I.; Bhattacharya, A. A.; Twine, S.; East, M.; Curry, S. *J Biol Chem* 2001, 276, 22804–22809.
40. Li, F.; Zhou, D.; Guo, X. *J Chromatogr Sci* 2003, 41, 137–141.
41. Kamal, J. K.; Zhao, L.; Zewail, A. H. *Proc Natl Acad Sci USA* 2004, 101, 13411–13416.
42. Carlson, H. A.; McCammon, J. A. *Mol Pharmacol* 2000, 57, 213–218.
43. Kumar, S.; Wolfson, H. J.; Nussinov, R. *IBM J Res Dev* 2001, 45, 499–512.
44. Korzekwa, K. R.; Krishnamachary, N.; Shou, M.; Ogai, A.; Parise, R. A.; Rettie, A. E.; Gonzalez, F. J.; Tracy, T. S. *Biochemistry* 1998, 37, 4137–4147.
45. Basurto, J. C.; Aburto, J.; Ferrara, J. T.; Torres, E. *Mol Model* 2007, 33, 649–654.
46. Artali, R.; Bombieri, G.; Calabi, L.; Del Pra, A. *Il Farmaco* 2005, 60, 485–495.
47. de Vries, S. J.; Bonvin, A. M. *Curr Protein Pept Sci* 2008, 9, 394–406.
48. Sudlow, G.; Birkett, D. J.; Wade, D. N. *Mol Pharmacol* 1976, 12, 1052–1061.
49. Mendieta-Wejebe, J. E.; Rosales-Hernández, M. C.; Rios, H.; Trujillo-Ferrara, J.; López-Pérez, G.; Tamay-Cach, F.; Ramos-Morales, R.; Correa-Basurto, J. *J Mol Model* 2008, 14, 537–545.
50. Rahman, M. H.; Yamasaki, K.; Shin, Y. H.; Lin, C. C.; Otagiri, M. *Biol Pharm Bull* 1993, 16, 1169–1174.
51. Sarver, R. W.; Gao, H.; Tian, F. *Anal Biochem* 2005, 347, 297–302.
52. Espinoza-Fonseca, L. M.; García-Machorro, J. *Biochem Biophys Res Commun* 2008, 370, 547–551.
53. Tulloch, L. B.; Morgan, H. P.; Hannaert, V.; Michels, P. A.; Fothergill-Gilmore, L. A.; Walkinshaw, M. D. *J Mol Biol* 2008, 383, 615–626.
54. Kortagere, S.; Krasowski, M. D.; Ekins, S. *Trends Pharmacol Sci* 2009, 30, 138–147.

*Reviewing Editor: J. A. McCammon*